ELECTROCHEMISTRY OF DOPAMINE β-HYDROXYLASE IN ADSORBED STATE AT A GOLD ELECTRODE

Ana ION[a], Torbjørn LJONES[b1] and Florinel G. BANICA[b2,*]

[a] *Department of Analytical Chemistry and Instrumental Analysis, University Politehnica of Bucharest, Romania; e-mail: ana_ion@chim.upb.ro*

[b] *Department of Chemistry, Norwegian University of Science and Technology, 7491 Trondheim, Norway; e-mail: [1] torbjorn.ljones@chem.ntnu.no, [2] f.banica@chem.ntnu.no*

Received September 3, 2003
Accepted January 7, 2004

Presented at the 36th Heyrovský Discussion on Electrochemistry of Biological Systems and Their Models.

Dopamine β-hydroxylase (DBH) adsorbed on gold electrode was investigated by electrochemical and quartz crystal microbalance methods. It was found that DBH can adsorb irreversibly on a gold electrode under open circuit conditions. In a neutral phosphate buffer, the adsorbed layer is stable to desorption within the potential range of 0.6 to –0.7 V vs Ag|AgCl (1 M KCl) electrode. At potentials positive than 0.8 V, adsorbed DBH undergoes an electrochemical oxidation involving probably tyrosine, tryptophan and histidine residues. This process is accompanied by DBH desorption and gold oxidation. In the cathodic potential region, from –0.2 to –0.7 V, DBH exhibits two reductions assigned to disulfide groups. No charge transfer reactions involving the copper centres in DBH have been noticed. However, DBH can bind reversibly copper(II) ions, which are not involved in the enzymatic activity and their presence was proved by voltammetry. The compactness of the adsorbed film was checked by cyclic voltammetry of selected redox probes at the DBH-coated electrode.
Keywords: Adsorption; Copper protein; Glycoproteins.

Dopamine β-hydroxylase[1–3] (DBH) (EC 1.14.17.1) is a copper enzyme which catalyzes a key hydroxylation step in the biosynthesis of noradrenaline and adrenaline. This compound acts as a main hormone and neurotransmitter in the nervous system. Bovine adrenal enzyme DBH, which was used in this work, is a glycoprotein with molecular weight ca. 290 kD, consisting of four identical subunits. Two pairs of monomers are assumed to be held together by disulfide bridges, and the pair bind to each other by non-covalent force. The whole molecule contains about 30 disulfide groups, but no thiol functions. The high contents of tyrosine (≈80 residues) and histidine (≈60 residues) provide a large number of oxidation-susceptible sites.

The three-dimensional structure of DBH has not yet been elucidated. However, some assumptions concerning the DBH structure can be made by analogy with the peptidylglycine α-hydroxylating monooxygenase (PHM) domain of peptidylglycine α-hydroxylating monooxygenase (E.C. 1.14.17.3), where PHM is mechanistically similar to DBH and its structure was already determined[4,5]. Thus, it has been inferred that each DBH molecule contains two copper centers that take part in the catalytic reaction like in the case of PHM. A careful investigation of copper binding in DBH was performed by Syvertsen et al.[6] who observed binding of up to four copper atoms per monomer. Abudu et al.[7] reported kinetic studies on the activation of DBH by copper ions and concluded that only one of these copper atoms is involved in catalysis. Other authors, however, have included both DBH and PHM in the class of noncoupled dinuclear copper proteins (for review see[8,9]). Here, the term "coupling" points to magnetic interaction between the copper centers. This implies that the distance between the Cu^{II} centers is of at least 0.7 nm and no ligand bridge exists.

It is obvious that, under properly selected conditions, a direct electron transfer to Cu^{II} centers in DBH may be expected. Such a process was thoroughly investigated for small copper proteins like copper-containing oxidases (see e.g.[10–27] and references therein).

This work deals with the electrochemistry of DBH irreversibly adsorbed on a gold electrode and may be, therefore, integrated within the field of protein-film voltammetry, as defined in[28,29]. In this context, the large molecular size of DBH is a particular feature. The gold electrode was used in this work because its surface can conveniently be modified in order to facilitate the electron transfer to redox proteins[28–33], particularly by the self-assembly method[34]. As a first step, we report here on the electrochemical behavior of DBH adsorbed on a bare gold surface. Our goal in this instance was to assess the stability and packing degree of the adsorbed layer. Also, the charge transfer reactions of DBH in the adsorbed state have been explored.

EXPERIMENTAL

DBH was extracted from bovine adrenal gland medulla, according to[3,35] and stored at –80 °C as an 8.7 mg/l solution in an aqueous phosphate buffer (pH 5). The DBH concentration was determined by spectrophotometry at 280 nm, according to[36]. After thawing at room temperature (20 ± 1 °C), a DBH sample was used within a maximum time period of 4 h.

Electrolyte solutions were prepared with fresh ultra-pure water (Millipore, specific resistance 18 MΩ cm). Potassium hexacyanoferrate(III) (Merck, p.a.), hexaammineruthenium(III) chloride (Strem Chemicals, 99%) and ferrocene-1,1′-dicarboxylic acid (Sigma, 96%) have

been used as redox probes. Other reagents were of analytical grade. All the experiments were performed in a phosphate buffer (26 mM Na_2HPO_4, 20 mM NaH_2PO_4, 0.1 M KNO_3, pH 7), if not stated otherwise.

A polycrystalline gold disk electrode was prepared by embedding a gold wire (Aldrich 99.99%, 1 mm diameter) in a glass tube with Epoxy resin. The electrode surface was conditioned by mechanical polishing followed by prolonged CV scanning in 0.01 M $HClO_4$ in the potential region from 0.00 to 1.45 V. An Ag|AgCl (1 M KCl) reference electrode was connected with the test solution via 1 M KNO_3 electrolyte bridge. The auxiliary electrode consisted of a platinum spiral. Other details in this respect are available in[37].

Protein adsorption onto the gold electrode surface was performed at room temperature (20 ± 1 °C) by dipping the electrode into a DBH solution. After a suitable time interval, the electrode was rinsed with deionized water, dried in N_2 stream and transferred into the voltammetric cell.

Voltammetric experiments have been performed at room temperature (20 ± 1 °C) with Autolab PGSTAT30 (Eco Chemie) equipment. Dissolved oxygen was removed from the test solution by bubbling with pure nitrogen until the oxygen reduction wave vanished. During recording, the nitrogen stream was directed above the solution. Fitting and simulation of the current–potential curves was performed with the Autolab GPES software.

For electrochemical quartz crystal microbalance (EQCM) measurements a Maxtek PM-710 plating monitor was used. The working electrode was a 5 MHz AT-cut quartz crystal (2.5 mm diameter), coated with a Ti-backed Au layer. Deposition of DBH on the piezoelectrode surface was performed by placing a layer of protein solution on the electrode surface held in horizontal position. After 1 h, the enzyme solution was removed, the gold surface was carefully rinsed with distilled water and the crystal was then placed in the voltammetric cell to record simultaneously the current and frequency shift.

RESULTS AND DISCUSSION

DBH Behavior in the Anodic Potential Region

Electrochemical behavior of DBH in the adsorbed state at a gold electrode shows features of a protein surface layer adsorbed on a noble metal surface[38]. As proved by Fig. 1a, curve *2*, the anodic current in the region of gold oxide formation (wave A) is larger for a DBH-coated electrode (curve *2*) compared with the plain gold electrode (curve *1*), although no difference appears in the gold oxide reduction peak (B). This demonstrates that additional charge on curve *2* associated with the anodic process is due to the oxidation of active groups in the adsorbed DBH molecule (such as tyrosine and tryptophan residues as well as cystine and histidine at extreme anodic potentials[38]).

The charge flowing during the first anodic scan (curve *2*, shoulder A) is by 35% higher than that recorded for the plain gold electrode (curve *1*). This difference diminishes to about 7% for the second scan (curve *3*), and is no more than ±2% for the following scans (curves *4* and *5*). This behavior may

be due both to the exhaustion of the oxidizable groups and protein desorption.

In order to distinguish between the described effects, EQCM was used to assess the mass change during the anodic process (Fig. 1b). Thus, in the potential region of the anodic reaction (Fig. 1b, curve *1*), a positive shift in the QCM frequency occurs (curve *2*) proving that the surface layer is removed during the anodic process. Subsequent scans do not display any noticeable frequency shift. At the same time, the absence of any negative frequency shift on the reverse branch of the curve *2* demonstrates that the DBH readsorption at less positive potentials cannot occur.

The change in frequency due to the gold oxide formation/reduction was beyond the detection limit under the conditions selected for recording mass change due to DBH desorption. Actually, the shift in frequency occurring on the first scan should be partially due to viscoelastic properties, the porous structure and entrapment of solvent molecules in the adsorbed film, as it is typical for protein layers[39]. Therefore, a direct relationship between the mass change and the frequency shift cannot be established. That is why no attempt was made to calibrate the QCM using the Sauerbray equation[40].

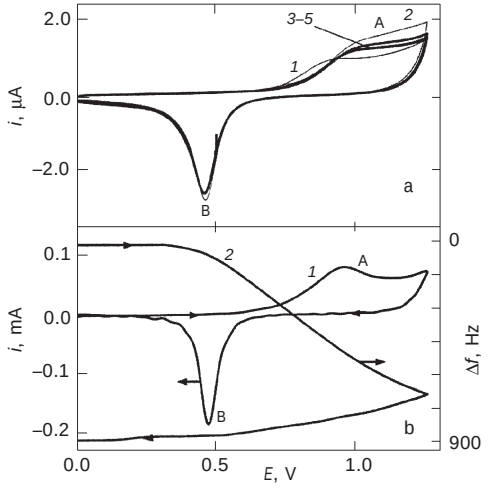

FIG. 1

Voltammetry of DBH-modified gold electrodes at positive potentials. a Cyclic voltammograms of bare Au-disk electrode (curve *1*) and successive CV scan at the DBH-modified electrode (curves *2–5*). Modification time 30 min, scan rate 50 mV s^{-1}. b Cyclic voltammogram (curve *1*) and smoothed EQCM frequency shift (curve *2*) measured at DBH-coated EQCM sensor (Au-coated). Adsorption time 60 min. Other conditions are as in a

Despite this limitation, the data in Fig. 1b prove that the surface layer was irreversibly desorbed during the anodic scan.

Curve *2* in Fig. 1b proves that the shift in frequency starts well before the onset of gold oxidation, in the so-called "pre-oxide" region[41]. Probably, the positive electrode potential induces some rearrangement in the adsorbed layer structure leading to modifications in its density and viscoelastic properties.

A further proof of DBH adsorption/desorption arises from the capacitive current determination in the double layer region (Fig. 2). A marked depression in the AC current occurs after performing the electrode modification (Fig. 2; curves *1* and *2*, respectively). In the frame of the Helmholtz model for the double layer, this behavior is accounted for by a combined effect of the thickness of the surface layer, which is much larger than the distance from the electrode to the Helmholtz plane in absence of adsorption. Also, the lower permittivity of the DBH layer may play an important role. However, the change in capacitance following DBH adsorption is much lower than that produced by a long-chain alkanethiol layer[42]. The difference may be due to water inclusion in the surface layer and also due to a stronger polarizability of the protein molecule.

Since the stoichiometry of the anodic oxidation is not clear, it is not possible to use the method stressed in[38] in order to assess the protein surface

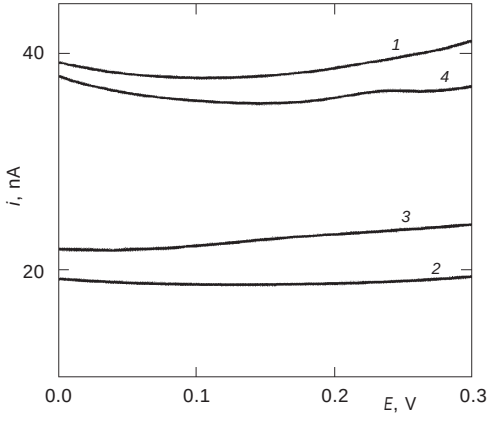

FIG. 2

Capacity current measurements by phase sensitive AC voltammetry (200 Hz, 5 mV rms, quadrature component). *1* Bare Au-disk electrode; *2* DBH-coated Au electrode; *3* the same electrode as in *2*, after performing a CV scan in the cathodic potential region of 0.15 to –0.70 V; *4* the same electrode as in *3*, after anodic desorption as in Fig. 1a

concentration. However, an analysis of adsorption kinetics was performed by assuming that the charge for the anodic oxidation process, Q_{ox}, is proportional to the surface concentration of DBH. The effect of the adsorption time on Q_{ox} provides the basis for the kinetic analysis of DBH adsorption. The charge Q_{ox} was calculated as follows:

$$Q_{ox} = \sum_{i=1}^{4} Q_{a,i} - 4\langle Q_5 \rangle . \qquad (1)$$

Here, $Q_{a,i}$ stands for the wave A charge (due to both protein and gold oxidation) on each of the 1st–4th scan, $\langle Q_5 \rangle$ represents the average charge recorded during the 5th scan for various modification times and is assigned to gold oxidation alone. In order to account for the variability in electrode surface area, Q_{ox} was further normalized to the peak B charge for the 5th scan (Q_c), which was assumed to be proportional to the electrode area

$$Q_{ox,n} = Q_{ox}/Q_c . \qquad (2)$$

For various adsorption times, ranging from 0 to 240 min, the $Q_{ox,n}$ vs t data fitted the Delahay–Trachtenberg relationship for diffusion-controlled adsorption[43] formulated as follows:

$$Q_{ox,n} = Q_l [1 - \exp(-bt)] . \qquad (3)$$

Here, t is in min and $Q_l = 1.84$ stands for the limiting value of $Q_{ox,n}$. The parameter $b = 0.017$ is a function of the adsorption constant in the linearized Langmuir isotherm, DBH diffusion coefficient and the thickness of the diffusion layer. A limiting surface coverage was attained after 30 min modification time and, consequently, this was the standard modification time throughout this work.

It results from what was said above that DBH adsorption under open circuit conditions is a diffusion-controlled process. During the anodic scan, the adsorbed DBH film undergoes an anodic oxidation accompanied by desorption within the region of the wave A. No attempt at investigating the adsorption isotherm was made because this approach is rendered inapplicable to the problem due to the irreversible character of the adsorption[44].

DBH Behavior in the Cathodic Potential Range

The first cathodic scan (potential range from +0.15 to –0.70 V; Fig. 3) displays the wave C with the halfwave potential $E_{1/2}$ = –0.30 V and the peak D with peak potential E_p = –0.60 V. Both of them are not present in subsequent scans and no anodic counterparts have been detected. These findings prove the irreversible character of the pertinent electrode processes.

The increase in the modification time results in an increase in the peak D current. At the same time, the wave C current experiences a slight depression. Under the same conditions, the charge for the overall cathodic process (both C and D processes) decreases to some extent (1.13, 1.07 and 1.00 μC for 15, 30 and 60 min modification time, respectively). Apparently, a longer modification time and higher packing degree lead to a molecule orientation that is less favorable to the wave C process.

In order to assess whether or not DBH desorption occurs during the cathodic scan, the capacity current was measured by AC voltammetry before (Fig. 2, curve *2*) and after performing a cathodic scan (Fig. 2, curve *3*). Accordingly, only a minor change in the capacity current arises after the cathodic scan proving that no significant desorption takes place under cathodic polarization. This conclusion is also supported by the results of an anodic desorption test (under the same conditions as in Fig. 1a), which followed a CV scan under the conditions of Fig. 3. Such a test resulted in a pattern

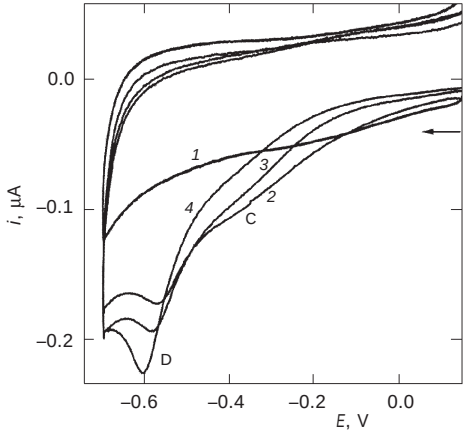

FIG. 3
Cyclic voltammetry of the Au|DBH electrode at negative potentials. Influence of the modification time (in min): *1* 0 (plain gold), *2* 17, *3* 30, *4* 65. Scan rate 50 mV s^{-1} (only the first CV scan is shown)

similar to that in Fig. 1a, curve *2*, and the corrected anodic charge (3.62 μC) was close to that recorded when the anodic desorption was performed without a prior cathodic scan (3.66 μA). Hence, it results that the cathodic currents in C and D arise from irreversible Faradaic processes that are not accompanied by major changes in the state of the adsorbed layer.

Data in Fig. 4 allow to assess whether or not a connection between the processes C and D exists. To this end, several successive CV scans have been performed with the same modified electrode but with different vertex potentials. The first scan was limited to the shoulder C region (Fig. 4, curve *1*), whereas the next scans (curves *2* and *3*) were extended to the negative limit of the potential window. The shoulder C is not evident on curve *2*, although peak D still appears. Both C and D processes do not arise on curve *3*, in accord with data in Fig. 3. It results, therefore, that these processes are independent of each other. The possible assumption that peak D is due to a product of process C is not supported by the chemical structure of DBH (see the last paragraph in this Section for details).

In order to assess the participation of copper centers in the cathodic reaction, the effect of copper removal from DBH by a strong chelator was investigated. To this end, the DBH-modified electrode was left for 30 min in contact with a 1 mM EDTA and then a CV scan was performed under the conditions of Fig. 3. The result (Fig. 5a) is similar to that in Fig. 3, indicating that

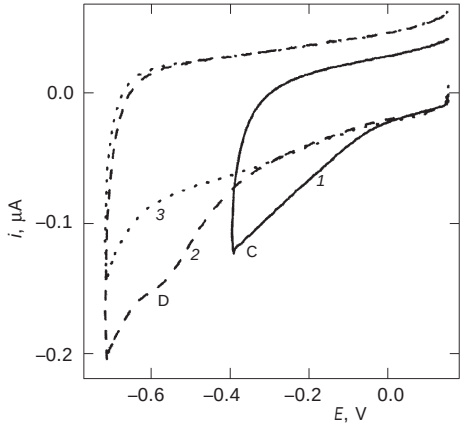

FIG. 4

Effect of the negative vertex potential. *1* CV scan in the potential region of wave C, *2* and *3* two successive scans in the potential region 0.2 to –0.7 V after performing the scan *1*. Modification time 30 min. Other conditions are as in Fig. 3

processes C and D cannot be assigned to the electron transfer involving copper centers in the enzyme.

The copper centers were thereafter reconstituted by leaving the modified electrode in contact with a 0.05 M Cu^{2+} solution for 3 min. The electrode was further carefully rinsed with distilled water and subjected to a CV scan in the anodic region (Fig. 5b, curve *1*). Patterns C and D, which vanished after the previous cathodic scan, do not reappear after the Cu^{2+} treatment. Instead, a couple of cathodic/anodic peaks develops ($E_{p,c}$ = 0.06 V, $E_{p,a}$ = 0.25 V), but vanishes after soaking the electrode in EDTA (Fig. 5b, curve *2*). This behavior reminds of the non-specific Cu^{2+} binding to DBH, as was already evidenced by potentiometry[6]. In view of these results, the voltammetric copper peaks in Fig. 5b may be assigned to copper ions attached to some sites that are different from the active Cu centers in the enzyme.

All the above results indicate that the patterns C and D cannot be assigned to electron transfer processes involving copper sites in DBH.

The nature of processes C and D can be elucidated if we bear in mind the occurrence of about 30 disulfide groups in the DBH molecule[3]. By analogy with proteins behavior at a mercury electrode[44], the reduction of disulfide groups should first be taken into account. On the other hand, it is necessary to remind that the disulfide interaction with the gold surface is a dissociative process and a reductive desorption process may occur as a con-

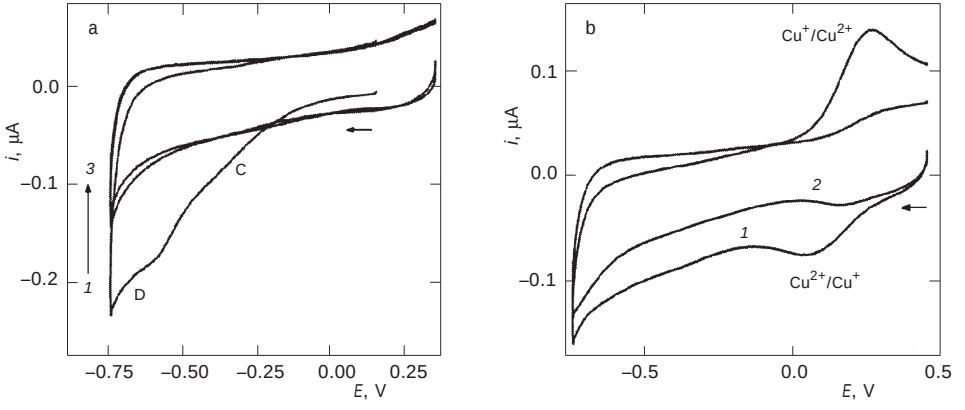

FIG. 5

Cyclic voltammetry of Au|Apo-DBH electrode. a Three successive CV scans in negative potential region. b Cyclic voltammetry after 3 min immersed in 5×10^{-2} M $CuSO_4$ solution (*1*); after 10 min in contact with 1×10^{-3} M EDTA solution (*2*). Modification time 30 min; scan rate 50 mV s^{-1}; supporting electrolytes: 26 mM Na_2HPO_4, 20 mM NaH_2PO_4, 0.1 M KNO_3; pH 7

sequence[12]. Experiments with cystine saturated solution in phosphate buffer, pH 7, yielded an irreversible cathodic peak located at –0.55 V (i.e., in the region of peak D). The cystine peak current is proportional to the scan rate (0.05–1.00 V s^{-1}), proving its surface character. According to[12], cystine interaction with gold surface results in a formation of adsorbed cystine layer which desorbs at –0.55 V in a reductive process. On the ground of the similarity of peak potentials, we assume that the DBH peak D corresponds to the reductive splitting of the sulfur–gold bonds. Such bonds form during the adsorption step by the dissociative surface interaction of exposed disulfide groups in DBH. Conversely, the wave C may be assigned to disulfide reduction on sites which are far enough from the metal surface to avoid its dissociative effect during the adsorption step. This interpretation is tentative but, at least, it is in accord with the data in Fig. 4 that demonstrate the absence of any influence of process C on the occurrence and intensity of peak D.

As the cathodic processes do not cause a major change in the surface state (Fig. 2, curves *2* and *3*), it can be concluded that the sulfur–gold interaction plays a minor role in the DBH adsorption which is dominated apparently by hydrophobic interactions.

Charge Transfer Reactions at the DBH-Coated Electrode

The electron-transfer reaction of various redox probes was investigated in order to evidence some properties of the adsorbed DBH layer, such as the compactness and packing degree. The selected probes were hexaammineruthenium(III) chloride, the hexacyanoferrate(III) ion and ferrocene-1,1′-dicarboxylic acid. A specific charge, molecular size, standard potential and standard rate constant for the electron transfer reaction characterizes each of them. Due to the polycrystalline structure of the gold electrode, it is highly probable that the adsorbed layer shows some structural imperfections even at a high-coverage degree. That is why the data interpretation was mostly based on the model of nonlinear diffusion to a partially blocked electrode[42,46,47]. According to this model, the charge transfer reaction may occur only at the exposed metal surface islands (pin-holes) and the electrode behaves as a microdisc electrode array (MEA). Deviations from this model may result from the partition of the probe between the adsorbed layer and the solution phase, as well as from electron tunneling or cooperative linear and spherical diffusion in the case of very small pin-hole[42].

Probe 1: $[Ru(NH_3)_6]^{3+}$

The $[Ru(NH_3)_6]^{3+/2+}$ charge transfer reaction is of the outer sphere type and proceeds with a very high rate constant; the standard exchange current density is of about 100 A cm^{-2} (see[48]). No difference between the voltammogram recorded at a plain gold electrode or at the same electrode after DBH adsorption was noticed up to a scan rate of 5 V s^{-1}. In both cases, the CV curve corresponds to a reversible process and displays the same peak parameters. This behavior is typical of a MEA with the average distance between two active centers being much lower than the thickness of the diffusion layer. This is the result of very high rate constant, which affords a fast expansion of the diffusion layer. At the same time, this demonstrates that the coverage degree is very close to unity.

Probe 2: $[Fe(CN)_6]^{3-}$

The use of $[Fe(CN)_6]^{3-}$ as a redox probe in CV may lead to confusing results due to the deterioration of the electrode surface by the formation of a polymeric hexacyanoferrate adsorbate[49]. That is why the stability of the CV response was assessed by series of five successive scans with only the first one displayed in each case. Also, long series of CV with the same electrode have been avoided.

The apparent standard rate constant for the $[Fe(CN)_6]^{3-/4-}$ couple is much lower than that for $[Ru(NH_3)_6]^{3+/2+}$ (see[50]). That is why, at the same time scale, the extension of the diffusion layer is more limited in the case of $[Fe(CN)_6]^{3-/4-}$. Consequently, the adsorbed film exerts a more important effect on the parameters of the CV curve (Fig. 6).

According to Fig. 6a, at a low scan speed the DBH film induces an increasing apparent irreversibility, as indicated by the simultaneous depression of peak currents and by increasing peak potential difference. According to the MEA model[46,47], this result demonstrates that the thickness of the diffusion layer is of the same order as the average distance between the active centers and, consequently, the linear and spherical diffusion occur to a comparable extent. However, at higher scan speed (Fig. 6b), the CV curve of the DBH-coated electrode (curve *2*) exhibits a marked asymmetry. Its cathodic branch approaches the shape of a steady-state irreversible curve, which is shifted to a higher overvoltage as compared with curve *1*. This indicates a spherical diffusion to active centers with almost no overlapping of diffusion layers. At the same time, the anodic branch (Fig. 6b, curve *2*) demonstrates a non-steady state typical of linear diffusion. The transition from the sym-

metrical shape (Fig. 6a, curve *2*) to the asymmetrical one (Fig. 6b, curve *2*) proceeds gradually with an increase in the scan rate. Rather than with the MEA model, this behavior may be accounted for by assuming a reactant partition between the solution and the adsorbed layer[51]. At high scan rates the transport process is mostly limited to the adsorbed layer, with no significant concentration profiles beyond its limit. The transport of $[Fe(CN)_6]^{3-}$ seems to proceed via preferred sites that behave like pin-holes, rendering the radial diffusion to be predominant. Conversely, $[Fe(CN)_6]^{4-}$ seems to partition, diffusing through the film, which behaves as a homogeneous medium.

It is clear that the behavior of $[Fe(CN)_6]^{3-/4-}$ at the DBH-coated electrode is too complicated to draw conclusions on the properties of the adsorbed film with certainty.

Probe 3: Ferrocene-1,1′-dicarboxylic Acid (FDA)

FDA behavior was investigated in a phosphate buffer in absence of potassium nitrate which may induce a marked instability of the FDA solution.

FDA reaction at a bare Au electrode (Fig. 7) has a quasireversible character, as proved by the ratio of the anodic/cathodic peak currents (1.004) and the peak separation (65 mV) measured at the 100 mV s^{-1} scan speed. Under

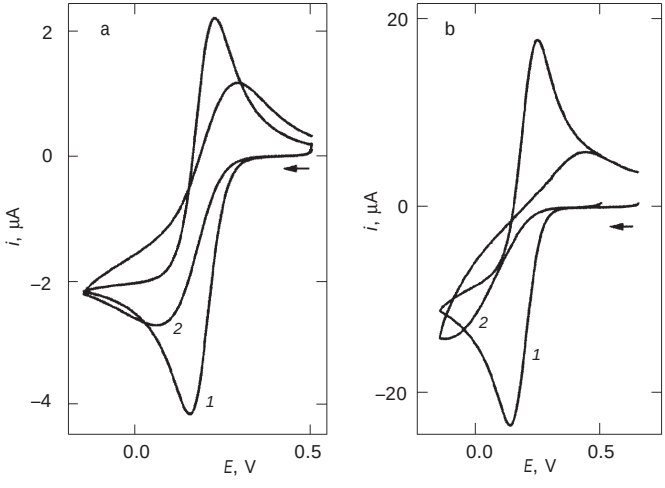

FIG. 6
CV response of 5 mM $[Fe(CN)_6]^{3-}$ in 0.1 M KNO_3 at plain Au (*1*) and the Au|DBH electrode (*2*). Scan rate (in mV s^{-1}): a 20, b 1000

the same conditions, the CV curve recorded at an Au/DBH electrode shows a higher degree of irreversibility; the peak separation is 0.125 V (Fig. 7a, curve *2*) but the anodic-to-cathodic peak current ratio remains close to unity. At a higher scan rate (Fig 7b), the voltammetric curve lost the peak shape, although the FDA reaction at the bare Au electrode preserved its quasi-reversible character (Fig. 7b, curve *1*).

An estimation of kinetic parameters for the FDA electron transfer reaction was made by a numerical fitting of the square-wave voltammetric curves (Fig. 8). The DBH adsorption brings about a significant drop in the apparent standard rate constant as well as an important decrease in the charge transfer coefficient. Combined with the CV data (Fig. 7), these results suggest that the DBH-coated surface behaves as an MEA towards the oxidation/reduction of negatively charged FDA redox species.

Series of CV experiments with FDA performed in potential region 0.2–0.6 V may lead to gradual inhibition of the electrode reaction, while simple contact of the DBH-coated electrode with the FDA solution does not have this effect. An extended cathodic sweep following a series of CV scans in the FDA reaction region reveals a new peak at –0.35 V and also removes the inhibition state. We assume that the ferricenium ion, formed by the oxidation of the ferrocene species, is destabilized upon iron co-ordination by ligand groups in DBH. Consequently, Fe(III) oxide (or hydrated hydroxide)

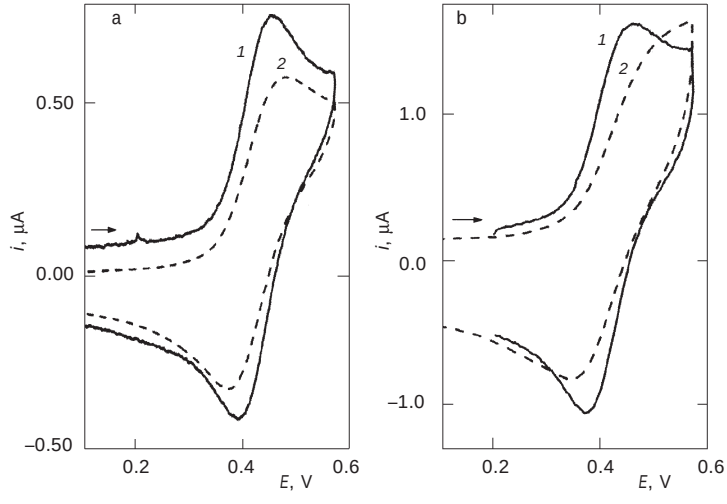

FIG. 7

Cyclic voltammograms of 0.5 mM FDA in 26 mM Na_2HPO_4 and 20 mM NaH_2PO_4. *1* Bare Au, *2* DBH-coated Au (modification time 30 min). Scan rate (in mV s^{-1}): a 100, b 10000

is formed and seals defects of the adsorbed layer. Fe(III) oxide reduction at –0.35 V restores the access of the solution to the free metal surface at the pin-hole defects. Ferricenium decomposition may occur by a mechanism similar to that proposed for ferricenium decay in the presence of OH^- and other inorganic anions[52].

The above mentioned inhibition process appears erratically, probably due to some uncontrollable variability in the structure of the surface layer. Data in Figs 7 and 8 have been gathered in the absence of such an effect. It results that the testing of protein surface layers by ferrocene-based redox probes must be done cautiously.

CONCLUSIONS

Electrochemistry of the DBH-adsorbed monolayer on polycrystalline gold surface was investigated by cyclic voltammetry, alternating current voltammetry, square wave voltammetry and electrochemical quartz crystal microbalance.

In a phosphate buffer at pH 7, the adsorption process is irreversible and proceeds under diffusion control. The DBH adsorption process is probably dominated by hydrophobic interactions. At the same time, some disulfide

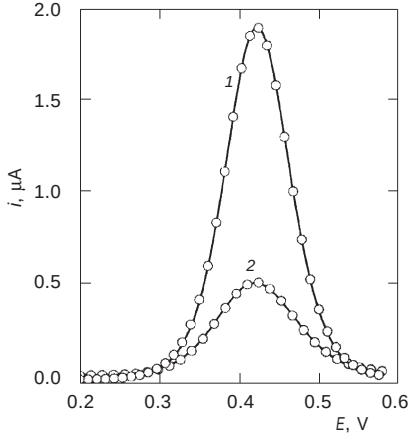

FIG. 8

Square wave voltammograms of 0.5 mM FDA. *1* Bare Au, *2* DBH-coated Au. Frequency 50 Hz, potential step 1.05 mV, amplitude 19.95 mV. Other conditions are as in Fig. 7. Lines, experimental values; circles, simulation. Parameters of simulation: E^0 = 0.42 V; apparent standard rate constant and transfer coefficient for curve *1*: 2.30×10^{-2} cm s^{-1} and 1, for curve *2*: 2.97×10^{-3} cm s^{-1} and 0.38; diffusion coefficient 1.86×10^{-6} cm^2 s^{-1} (determined from the FDA CV curve at a plain gold electrode); T = 293 K

groups interact in a dissociative way with gold surface to form thiolate–gold bonds.

In the anodic region, the adsorbed layer is stable up to 0.7 V vs the Ag|AgCl (1 M KCl) reference electrode. At more positive potentials, DBH oxidation and desorption occur at the same time with gold oxidation. In the cathodic potential region (up to –0.7 V), the DBH layer is relatively stable to desorption. However, two irreversible and not interconnected cathodic processes have been identified at –0.30 and –0.55 V and assigned to the reduction of disulfide groups and reductive splitting of the gold–thiolate bonds, respectively. No direct electron transfer involving the active copper centers in the enzyme was detected. On the other hand, the copper ion binds reversibly to some non-specific sites in DBH and is electrochemically active in this form.

Electron transfer reactions of selected redox probes suggest that the DBH-adsorbed layer is not completely impermeable to $[Ru(NH_3)_6]^{3+}$, $[Fe(CN)_6]^{3-}$, or FDA. In the case of $[Ru(NH_3)_6]^{3+}$ and FDA, the mass transfer through the surface film is localized at small defects and the DBH-coated electrodes behave as an ultramicroelectrode array. In the case of $[Fe(CN)_6]^{3-}$, reactant partition between the surface layer and the solution phase may complicate the overall process.

The presented results referring to DBH adsorption may be of relevance when attempting to perform DBH immobilization at a modified gold electrode. In such an instance, strong DBH interaction with the metal surface may lead to competitive adsorption and more or less advanced substitution of the modifier by DBH.

A. Ion gratefully acknowledges financial support of the Norwegian Research Council. The authors are indebted to Dr B. Børresen (Department of Material Technology, NTNU) for access to EQCM and assistance at measurement and to K. Ljones for technical assistance in purification of enzyme.

REFERENCES

1. Skotland T., Ljones T.: *Inorg. Persp. Biol. Med.* **1979**, *2*, 151.
2. Ljones T., Skotland T. in: *Copper Proteins and Copper Enzymes* (R. Leontie, Ed.), p. 132. CRC Press, Boca Raton 1984.
3. Ljones T.: *Methods Enzymol.* **1987**, *12*, 596.
4. Prigge S. T., Kolhekar A. S., Eipper B. A., Mains R. E., Amzel L. M.: *Science* **1997**, *278*, 1300.
5. Prigge S. T., Mains R. E., Eipper B. A., Amzel L. A.: *Cell. Mol. Life Sci.* **2000**, *57*, 1236.
6. Syvertsen C., Gaustad R., Schrøder K., Ljones T.: *J. Inorg. Biochem.* **1986**, *26*, 63.
7. Abudu N., Banjaw M. Y., Ljones T.: *Eur. J. Chem.* **1998**, *257*, 622.

8. Solomon E. I., Chen P., Metz M., Lee S.-K., Palmer A. E.: *Angew. Chem., Int. Ed.* **2001**, *40*, 4570.
9. Klinman J. P.: *Chem. Rev.* **1996**, *96*, 2541.
10. Rooney M. B., Honeychurch M. J., Selvaraj F. M., Blankenship R. E., Bond A. M., Freeman H. C.: *J. Biol. Inorg. Chem.* **2003**, *8*, 306.
11. Jeuken L. J. C., Wisson L. J., Armstrong F. A.: *Inorg. Chim. Acta* **2002**, *331*, 216.
12. Zhang J., Chi Q., Nielsen J. U., Hansen A. G., Andersen J. E. T., Wackerbarth H., Ulstrup J.: *Russ. J. Electrochem. (Transl. of Elektrokhimiya)* **2002**, *38*, 68.
13. Jeuken L. J. C., McEvoy J. P., Armstrong F. A.: *J. Phys. Chem. B* **2002**, *106*, 2304.
14. Lisdat F., Karube I.: *Biosens. Bioelectron.* **2002**, *17*, 1051.
15. Zhang J., Chi Q., Kuznetsov A. M., Hansen A. G., Wackerbarth H., Christensen H. E. M., Andersen J. E. T., Ulstrup J.: *J. Phys. Chem. B* **2002**, *106*, 1131.
16. Jeuken L. J. C., Armstrong F. A.: *J. Phys. Chem. B* **2001**, *105*, 5271.
17. Battistuzzi G., Borsari M., Canters G. W., de Waal E., Loschi L.,Warmerdam G., Sola M.: *Biochemistry* **2001**, *40*, 6707.
18. Fristrup P., Grubb M., Zhang J., Christensen H. E. M., Hansen A. M., Ulstrup J.: *J. Electroanal. Chem.* **2001**, *511*, 128.
19. Chi Q. J., Zhang J. D., Andersen J. E. T., Ulstrup J.: *J. Phys. Chem. B* **2001**, *105* 4669.
20. Chi Q. J., Zhang J. D., Nielsen J. U., Friis E. P., Chorkendorff I., Canters G. W., Andersen J. E. T., Ulstrup J.: *J. Am. Chem. Soc.* **2000**, *122*, 4047.
21. Forzani E. S., Solis V. M., Calvo E. J.: *Anal. Chem.* **2000**, *72*, 5300.
22. Chi Q. J., Zhang J. D., Friis E. P., Andersen J. E. T., Ulstrup J.: *Electrochem. Commun.* **1999**, *1*, 91.
23. Battistuzzi G., Borsari M., Loschi L., Righi F., Sola M.: *J. Am. Chem. Soc.* **1999**, *121*, 501.
24. Battistuzzi G., Borsari M., Loschi L., Sola M.: *J. Inorg. Biochem.* **1998**, *69*, 97.
25. Santucci R., Ferri T., Morpurgo L., Savini I., Avigliano L.: *Biochem. J.* **1998**, *332*, 611.
26. Yaropolov A. I., Kharybin A. N., Emneus J., MarkoVarga G., Gorton L.: *Bioelectrochem. Bioenerg.* **1996**, *40*, 49.
27. Jeuken L. J. C., Wisson L. J., Armstrong F. A.: *Inorg. Chim. Acta* **2002**, *331*, 216.
28. Armstrong F. A., Heering H. A., Hirst J.: *Chem. Soc. Rev.* **1997**, *26*, 169.
29. Armstrong F. A.: *J. Chem. Soc., Dalton Trans.* **2002**, 661.
30. Armstrong F. A.: *Electrochim. Acta* **2000**, *45*, 2623.
31. Armstrong F. A.: *Struct. Bond.* **1990**, *72*, 137.
32. Guo L.-H., Hill H. A. O.: *Adv. Inorg. Chem.* **1991**, *36*, 341.
33. Armstrong F. A., Hill H. A. O., Walton N. J.: *Acc. Chem. Res.* **1988**, *21*, 407.
34. Creager S. E., Olsen K. G.: *Anal. Chim. Acta* **1995**, *307*, 277.
35. Ljones T., Skotland T., Flatmark T.: *Eur. J. Biochem.* **1976**, *61*, 525.
36. Ljones T., Skotland T.: *Int. J. Pept. Protein Res.* **1977**, *10*, 311.
37. Ion A., Partali V., Sliwka H. R., Banica F. G.: *Electrochem. Commun.* **2002**, *4*, 674.
38. Roscoe S. G. in: *Modern Aspects of Electrochemistry* (J. O'M Bockris, B. E. Conway and R. E. White, Eds), Vol. 29, p. 319. Plenum Press, New York 1996.
39. Rodahl M., Höök F., Fredriksson C., Keller C. A., Krozer A., Brzezinski P., Voinova M., Kasemo B.: *Faraday Discuss. Chem. Soc.* **1997**, *107*, 229.
40. Buttry D. A., Ward M. D.: *Chem. Rev.* **1992**, *92*, 1355.
41. Tüdös A. J., Vandenberg P. J., Johnson D. C.: *Anal. Chem.* **1995**, *67*, 552.
42. Finklea H. O. in: *Electroanalytical Chemistry* (A. J. Bard and I. Rubinstein, Eds), Vol. 19, p. 109. Marcel Dekker, New York 1996.

43. Delahay P., Trachtenberg I.: *J. Am. Chem. Soc.* **1957**, *79*, 2355.
44. Ramsden J. J.: *Q. Rev. Biophys.* **1993**, *27*, 41.
45. Honeychurch M. J.: *Bioelectrochem. Bioenerg.* **1997**, *44*, 13.
46. Amatore C., Saveant J. M., Tessier D.: *J. Electroanal. Chem., Interfacial Electrochem.* **1983**, *147*, 39.
47. Lipkowski J. in: *Modern Aspects of Electrochemistry* (J. O'M Bockris, B. E. Conway and R. E. White, Eds), Vol. 23, p. 1. Plenum Press, New York 1992.
48. Iwasita T., Schmickler W., Schultze J. W.: *Ber. Bunsen–Ges. Phys. Chem.* **1985**, *89*, 138.
49. a) Pharr C. M., Griffiths P. G.: *Anal. Chem.* **1997**, *69*, 4665; b) Oslonovitch J., Li Y.-J., Donner C., Krischer K.: *J. Electroanal. Chem.* **2003**, *541*, 163.
50. Iwasita T., Schmickler W., Herrmann J., Vogel U.: *J. Electrochem. Soc.* **1983**, *130*, 2026.
51. Markovich I., Mandler D.: *J. Electroanal. Chem.* **2000**, *484*, 194.
52. Holeček J., Handlíř K., Klikorka J.: *Collect. Czech. Chem. Commun.* **1979**, *44*, 1379.